Available online at www.sciencedirect.com

ScienceDirect

Ceramics International 40 (2014) 763–770

CERAMICS INTERNATIONAL

www.elsevier.com/locate/ceramint

Lighter tableware ceramic by controlling porosity: Effect of porosity on mechanical properties

Benjamin Verhaeghe[a,b], Christian Courtois[a,b,*], F. Petit[d], F. Cambier[d], Jean-Dominique Guérin[a,c], Anne Leriche[a,b], Stuart Hampshire[e]

[a]Univ Lille Nord de France, F-59000 Lille, France
[b]UVHC, LMCPA EA 2443, F-59313 Valenciennes, France
[c]UVHC, TEMPO EA 4542, F-59313 Valenciennes, France
[d]Belgian Ceramic Research Centre, B-7000 Mons, Belgique
[e]Materials and Surface Science Institute, University of Limerick, Limerick, Ireland

Received 12 June 2013; received in revised form 18 June 2013; accepted 18 June 2013
Available online 27 June 2013

Abstract

Reduction in weight of ceramics has been achieved by using a specific porous agent, starch, to achieve porosity ranging from 10% to 35%. Two incorporation routes of the porous agent have been investigated. For different levels of weight reduction, ceramics are characterized by microstructural analysis and mechanical testing. It is shown that the feature of the porous phase mainly depends on the processing route. Two step route leads to the best microstructures and allows ceramics be made up to ten percent lighter without impacting compressive strength (380 MPa) and similar to matrix but with larger variation.

Keywords: B. Porosity; C. Mechanical properties; Lighter tableware ceramic; Microstructure; Sustainable porous agent

1. Introduction

For ceramics, lightness in weight [1], thermal [2–4] and acoustic insulation are characteristics that can be obtained by means of some controlled porosity addition [5–10]. The addition of such porosity generally leads to some decrease in mechanical properties due to the formation of larger defects in the body [11–16]. The aim of this study is to develop porous ceramic tableware. Addition of well controlled porosity in terms of shape, size and spatial distribution will minimize the decrease of the lighter ceramic mechanical properties. In this work, the addition of porosity is realized through the use of starch. The targeted weight reduction value is 10%, relative to the initial matrix. Two porous agent incorporation routes are investigated as explained in the next section. Mechanical properties of the lighter materials obtained are determined and analyzed relative to the porosity, microstructures and processing routes. The proposed solution has the advantage of being compatible with industrial processes while using a natural and sustainable porous agent.

2. Experimental methods

2.1. Raw materials

Matrix. It consists of a classical tableware formulation based on a clay–silica–alumina–feldspar mixture supplied in an atomized form. Fig. 1(a) presents a SEM micrograph of atomized agglomerates. They exhibit some hollow spherical shape, with an average diameter of 250 μm.

Porous agent. The used porous agent is a corn starch. It exhibits a thermoplastic behavior below its glass transition temperature (65–68 °C). Fig. 1(b) presents SEM observation of this porous agent. It exhibits some spherical shape with a narrow particle size distribution. d_{50} value is 11 μm, while the

*Corresponding author at: UVHC, LMCPA EA 2443, F-59313 Valenciennes, France. Tel.: +33 327531669.
E-mail address: christian.courtois@univ-valenciennes.fr (C. Courtois).

0272-8842/$ - see front matter © 2013 Published by Elsevier Ltd and Techna Group S.r.l.
http://dx.doi.org/10.1016/j.ceramint.2013.06.066

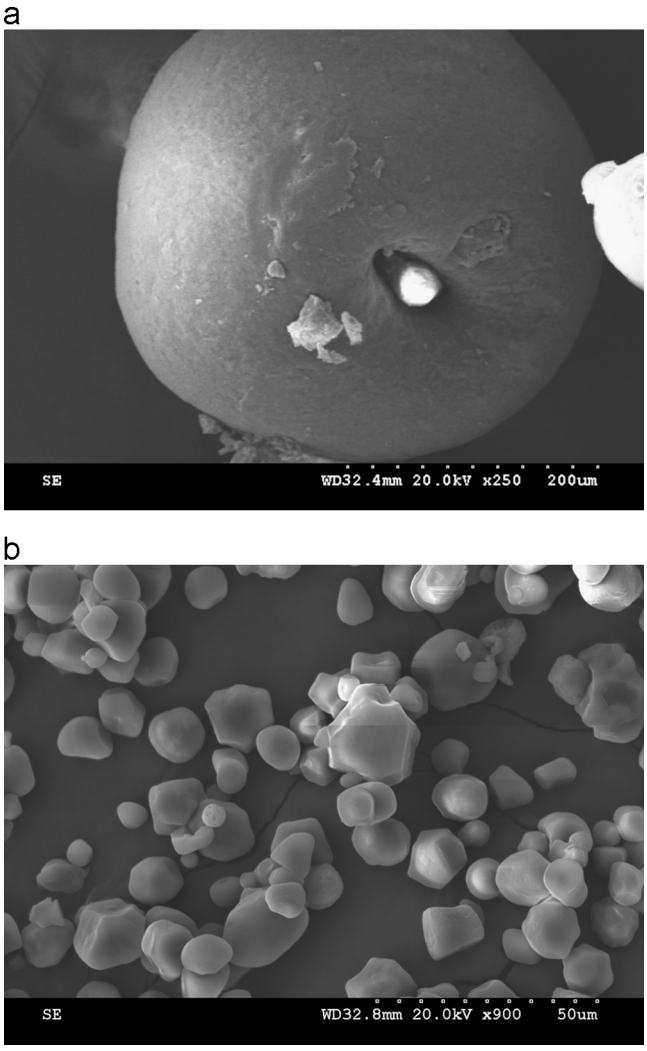

Fig. 1. SEM micrographs of the ceramic powder (a) and the porous agent (b).

d_{10} and d_{90} values are, respectively, 8 and 15 μm. This porous agent is natural and can be easily integrated into the conventional ceramic process. It would lead to the generation of tailored porosity after its degradation during the sintering of the ceramic powder.

2.2. Processing routes

Fig. 2 presents a flowchart describing the different processing routes developed in this study. The main differences concern the powder preparation step.

The first route, called the One-step route, consists in a simple dry mixing of atomized powder with various amounts of porous agent. The powders are mixed for 1 h (Turbula®). Ten cylindrical zirconia mixing media pellets with 10 mm length and 10 mm diameter are used per batch of 200 g of powder. The second route, called the Two-step route, consists in finely mixing the ceramic powder and the porous agent in a slurry prior to its atomization. Fig. 3 shows a SEM observation of a cut aggregate. It can be seen that after the atomization step, the starch is not crushed. It is homogeneously dispersed in the aggregate. If compared to the non starch-containing

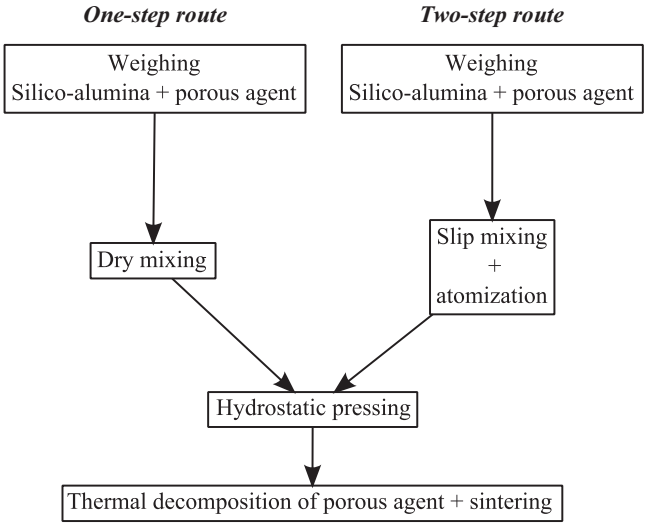

Fig. 2. Flowchart of the different tested routes.

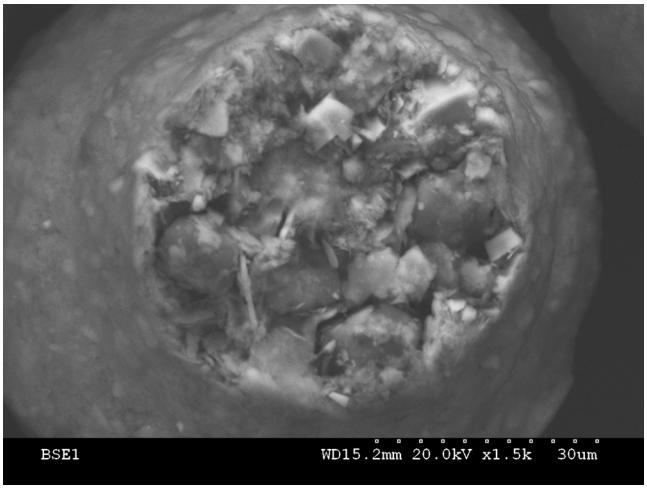

Fig. 3. SEM observation of 12% atomized powder with porous agent.

atomized ceramic powder (Fig. 1(a)) it can be observed that the addition of corn starch into the raw powder modifies the atomization conditions in such a way that no more agglomerate internal porosity is generated (Fig. 3). Therefore, it might be expected that such mixed agglomerates could lead to the synthesis of finely porous materials.

Shaping procedures and sintering conditions are the same for both of the investigated routes. Dry pressing is realized under 30 MPa hydrostatic pressure. A classical sintering cycle has been used for all studied samples: heating up to 60 °C at 1 °C/min followed by a holding time of 6 h; a second heating up to 250 °C at 1 °C/min followed by a holding time of 2 h, a rapid heating up to 1380 °C at 5 °C/min followed by a holding time of 2 h, and finally a decrease to room temperature at 5 °C/min. The first two steps correspond respectively to the drying and degradation of the porous agent. The final step enables the sintering of the parts. A reference matrix is fabricated from atomized ceramic powder without starch.

3. Characterization methods

3.1. Physical and microstructural characterization

Density. Density measurements are performed by hydrostatic weighing using the Archimedes method under water. Measurements are performed on a series of 10 samples. Values presented are the average of these 10 measurements expressed as a function of relative density ($d_0 = 2550$ Kg/mm^3 determined by He picnometry measurements) in order to determine volume% porosity.

Scanning electron microscopy observations. Observations of powders were carried out by using a scanning electron microscope HITACHI S-3500N. The observed powders are deposited on a sample holder covered with graphite paper and a gold film is sputtered before observation.

Mercury porosimetry. Porosity measurements are performed with a mercury porosimeter Quantachrome Poremaster 33GT. Samples with 8 mm diameter and 10 mm length are introduced into a glass holder. Some mercury is introduced under pressure varying between 0.006 and 0.344 MPa. Accessible open pore size ranges from 4.3 to 225.6 μm.

3.2. Mechanical characterization

Compressive strength. Measurements are performed on an INSTRON universal testing machine. The displacement is applied with a crosshead speed of 2 mm/min. For such loading speed conditions, quasi-static deformation occurs. This compression test requires massive parts in the form of cylinders with 10 mm diameter and a height between 15 mm and 25 mm to prevent some bulking phenomenon. These shapes and dimensions are obtained from samples by drilling and 2 μm diamond polishing to ensure a good parallelism between the upper and lower radial sides of the specimen. A minimum of 10 measurements are carried out on each material and the average is calculated.

Bending strength and toughness measurements. Four point bending tests are performed on a ZWICK Z100 universal testing machine. Several prismatic parts with a cross section of 4 mm in width and 3 mm in height are prepared by cutting and polishing as above for the compressive test samples. The same geometry of specimens are subsequently used for toughness determination by the Single Edge V-Notched Beam (SEVNB) method. This method uses a razor blade with diamond paste to introduce a final notch with a root radius between 10 and 20 μm and a depth of about 1 mm. The samples are then fractured in a three-point bending test using a universal testing machine (crosshead speed of 0.1 mm/min). A minimum of 15 measurements is realized on each material and the average value is calculated.

4. Results and analysis

4.1. Microstructures

Denser ceramic. Fig. 4 presents SEM observation of the sintered matrix after polishing. Relative density is 92% of theoretical (2550 Kg/mm^3). It can be observed that agglomerates have not been totally crushed after pressing so that the ceramic is not totally densified during the sintering step. Residual porosity is mainly closed and both inter- and intra-agglomerate pores remain. Larger pores with a diameter size of about 70 μm are located inside the remaining atomized spheres.

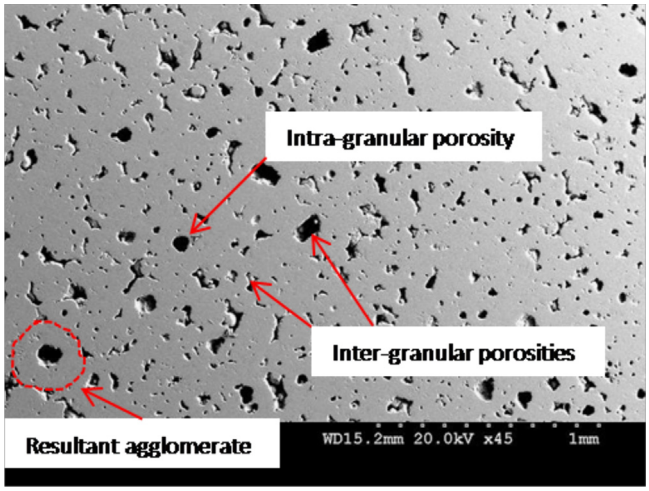

Fig. 4. SEM micrograph, ceramic reference matrix after sintering (residual porosity 8%).

Lighter ceramics using the One-step route. Fig. 5(a) presents for the One-step route the variation of total, closed and open porosity as measured on different samples containing different amounts of starch. SEM observations (Fig. 6) show that atomization aggregates are partially crushed and do not depend on the amount of added porous agent. Two types of porosity remain: intra- and inter-agglomerate pores. Samples with addition of 5% of porous agent exhibit some porosity of 10 μm diameter distributed around aggregates of atomization, in addition to the residual porosity in the matrix after sintering (Fig. 6(a)). If 10% of porous agent is introduced, intra-granular porosity remains, while the inter-granular pore size increases up to 12 μm (Fig. 6(b)). Large pores are likely generated by coalescence favoring an interconnection of pores as the amount of porous agent increases. Percolation occurs when greater than 4% addition of porous agent is used. At the same time, the closed pore volume increases. An improvement of the pore size distribution is observed at the percolation threshold (SEM micrograph Fig. 6(c)). The porosity is then mostly open and interconnected. These results are confirmed by Hg intrusion measurements (Fig. 5(b)). The size of the porosity drastically increases with addition of starch as soon as the percolation threshold is overcome. Then, a secondary peak corresponding to two or three times the size of the pores created by the porous agent appears. Above 10% of added porous agent, a significant broadening of the pore size distribution is observed.

Lighter ceramics by using the Two-step route. Fig. 7 presents for the Two-step route the changes in total, closed and open porosity as measured on different samples containing different amounts of the introduced porous agent. SEM micrographs of cross sections of the most typical samples

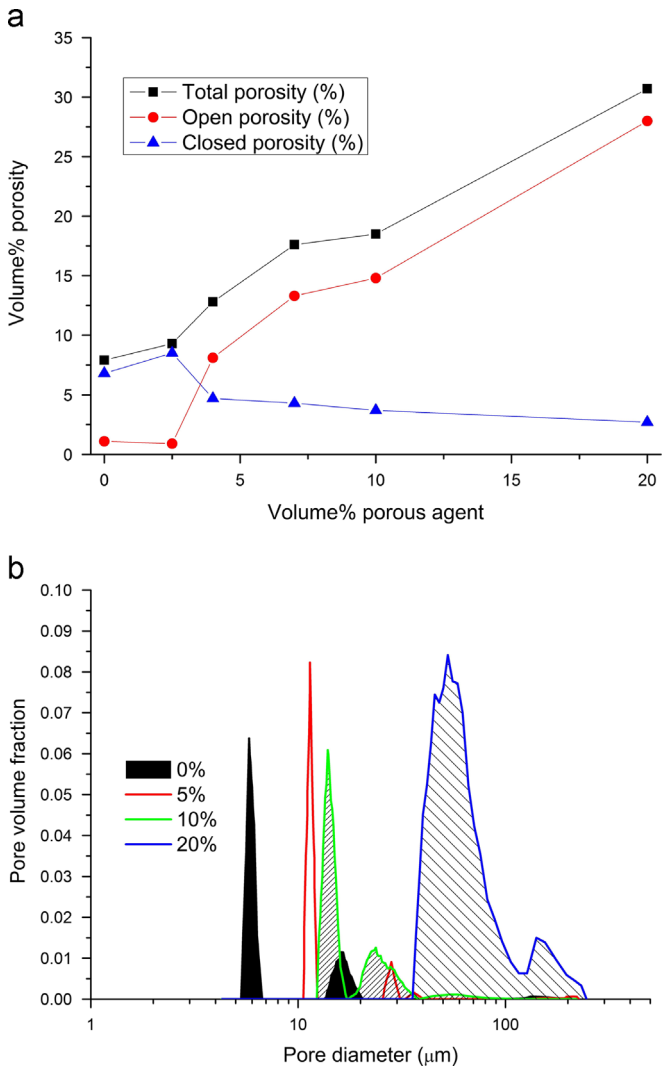

Fig. 5. One-step route: influence of the added amount of porous agent on (a) resulting porosities and (b) resulting open porosity.

after polishing are presented in Fig. 8. The same trends are observed when compared to the One-step route results. The addition of porous agent promotes an increase of closed porosity up to 12 vol% added starch, and the variation of total porosity with the amount of added porous agent follows a linear trend indicating that the created porosity is nearly additive to the residual porosity in the matrix after sintering. A limited addition of porous agent (8 vol%) favors a diminution of the initial intra-granular porosity and promotes the formation of a finely porous material (Fig. 8(a)). For higher additions of starch, aggregation of porosity occurs leading to a coarser pore structure (Fig. 8(c)). The size of the pores increases significantly as soon as coalescence occurs and pore size reaches 100 μm for 18 vol% of introduced porous agent. The porosity remains homogeneously distributed whatever the amount of added porous agent. For this route, the percolation threshold occurs at a higher amount (15 vol%) of added starch and therefore higher total porosity. This is probably due to better pores size distribution induced by the use of atomized spheres containing starch.

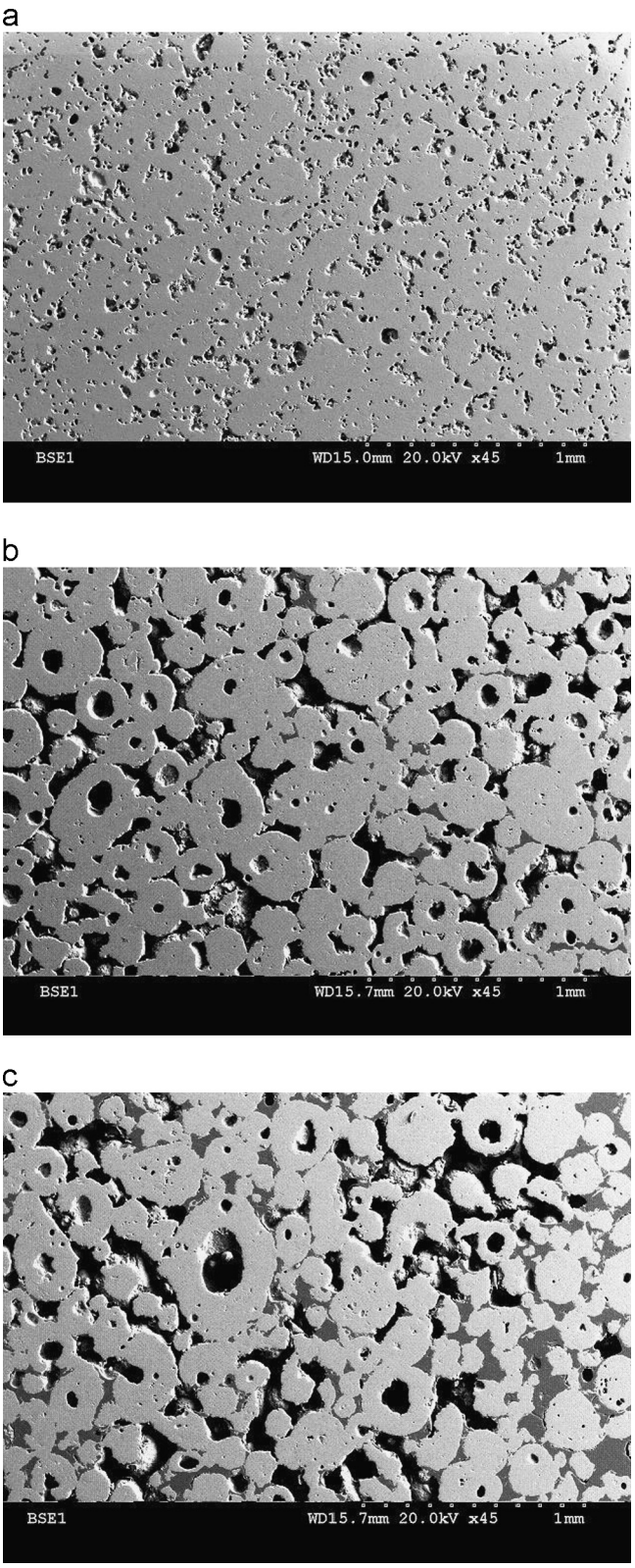

Fig. 6. One-step route, SEM micrographs of sintered ceramics containing (a) 5%, (b) 10% and (c) 15% of added porous agent.

4.2. Mechanical properties

Matrix. Mechanical properties of the sintered material without porous agent are a compressive strength value of

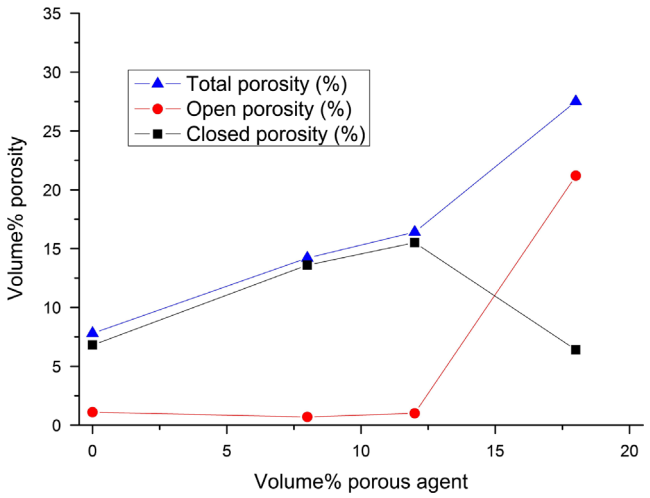

Fig. 7. Two-step route: influence of the amount of added porous agent on the resulting porous phase.

290 ± 90 MPa, a bending strength value of 85 ± 5 MPa and a toughness value of 1.12 ± 0.02 MPa$\sqrt{m}$. Large pores act as critical defects explaining the limited values of compressive and flexural strengths. By using Griffith's equation, starting from average values of measured bending strength and toughness, a critical defect size of about 54 μm is calculated. It is comparable to the larger pore size which was determined from porosimetry and SEM observations.

One-step route. Fig. 9 presents the values of compressive strength and bending strength determined for the different parts. By comparing these materials to the matrix, a slight decrease of compressive strength from 290 ± 90 MPa (≈8% total porosity) to 200 ± 40 MPa (≈18% total porosity) occurs with the increase in porosity. At the percolation threshold (≈12% of total porosity), compressive strength appears similar to the matrix sample but with larger standard variations. At 18% total porosity, strength values are close to those obtained with a small addition (2.5 vol%) of porous agent. Considering standard variation values, the compressive strength discrepancies are high. From a technical point of view, this type of characterization is difficult since perfect parallelism of both flat end surfaces of the cylinder is not systematically obtained. Moreover, some friction between specimen and apparatus can occur and probably depends on the level of porosity in the sample external surfaces. For that reason, compressive strength results must be treated cautiously. Nevertheless, it seems that observed compressive strength values decrease significantly above the percolation threshold. Bending strength values decrease continuously (from 90 ± 5 MPa to 20 ± 2 MPa) as porosity increases (from ≈8% to ≈18% of total porosity). As with compressive strength, a similar trend is observed, with large decrease in bending strength on addition of a small amount (2.5 vol%) of porous agent followed by an apparent stabilization up to 4 vol% starch and then a slight decrease for the lighter ceramics. Bending strength measurements exhibit fewer discrepancies when compared to compressive strength measurements with significantly lower standard deviation values for the more porous ceramic which is probably due to

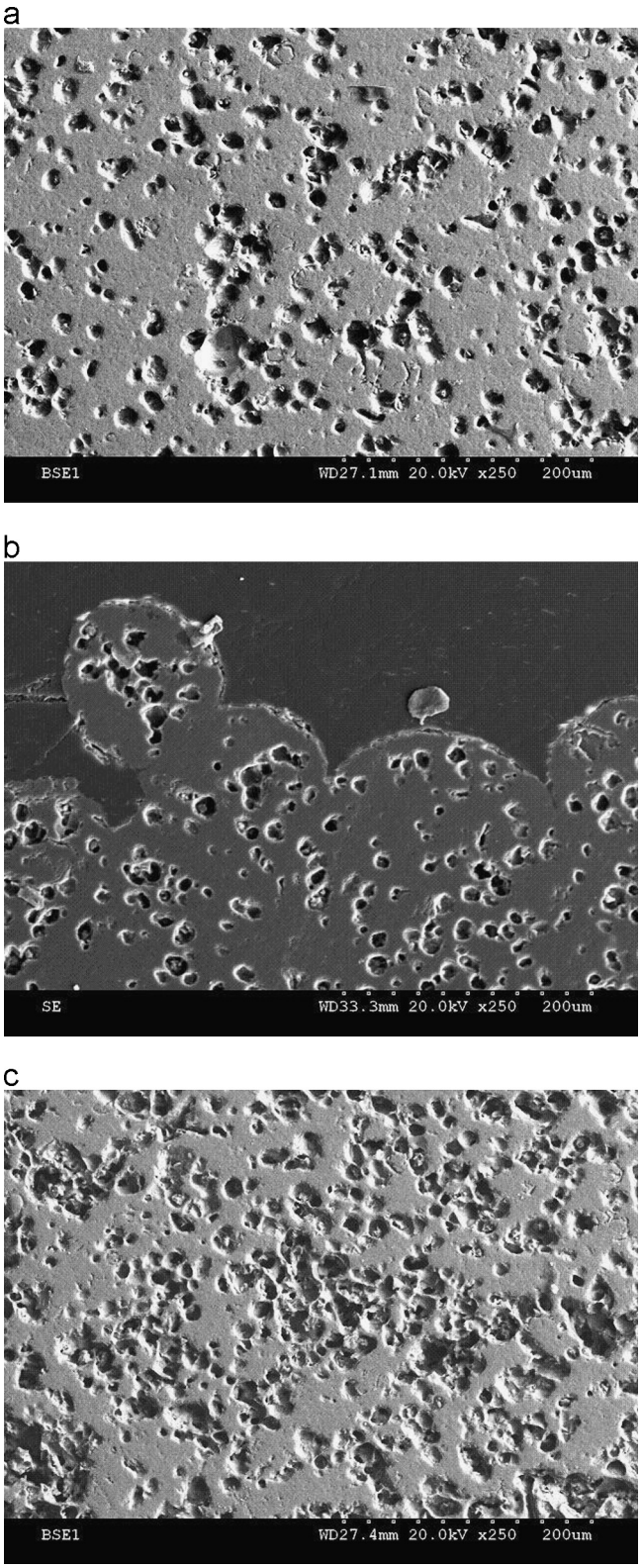

Fig. 8. Two-step route, SEM micrographs of sintered ceramics containing (a) 8%, (b) 12% and (c) 18% of added porous agent.

better distributed porosity leading to more repeatable mechanical behavior. Variation of toughness with amount of porosity is presented in Fig. 10 which also plots calculated critical flaw size values (after Griffith's equation) as a function of porosity.

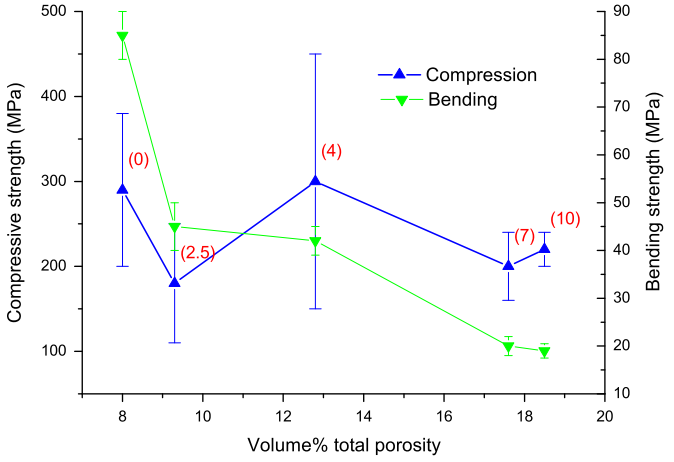

Fig. 9. One-step route: mechanical strength vs the total porosity in lighter ceramics; in (✻) the volume% of added porous agent.

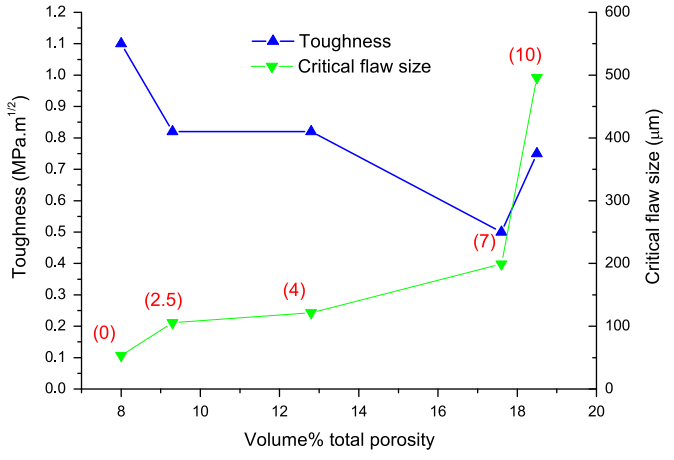

Fig. 10. One-step route: toughness and calculated critical flaw size vs the total porosities in lightened ceramics, in (✻) the volume amount of added porous agent.

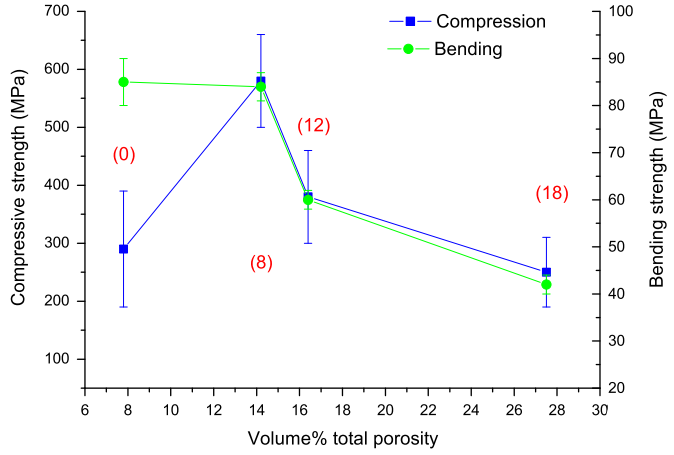

Fig. 11. Two-step route: mechanical strength vs the total porosity in lighter ceramics; in (✻) the volume% of added porous agent.

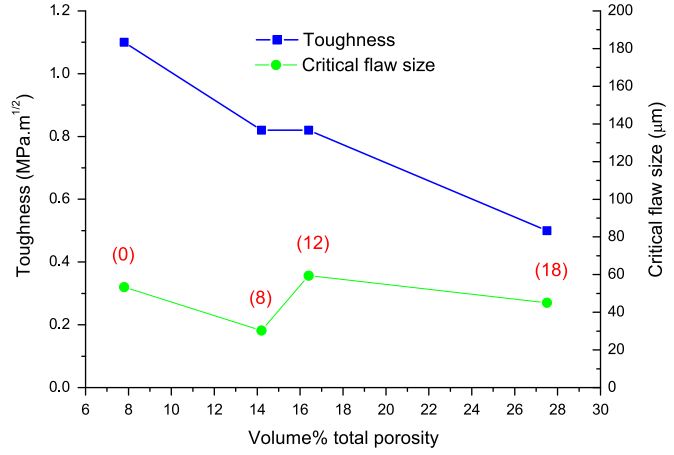

Fig. 12. Two-step route: toughness and calculated critical flaw size vs the total porosity in lighter ceramics; in (✻) the volume% of added porous agent.

The introduction of 2.5 vol% of the porous agent leads immediately to a toughness decrease from 1.12 ± 0.02 to 0.82 ± 0.05 MPa$\sqrt{m}$. A slight stabilization is observed just before the percolation threshold. The critical flaw size values slightly increase with starch addition up to 7 vol% then increase significantly with further addition. For all the ceramics, the value of the critical flaw size is of the same order of magnitude as the size of the largest pore created. As can be observed in SEM micrographs (Figs. 4 and 6), below 7 vol% of added porous agent, coarsening of pores is not significant. Added pores are mainly localized around the remaining matrix aggregates without interaction with the residual porosity after sintering. On the contrary, for most of the lighter ceramics, added pores merge together explaining the huge increase in the critical flaw size. At the same time, some toughening is observed and is probably due to some crack deviation phenomenon [17,18].

Two-step route. In Fig. 11 are presented the values of compressive strength and bending strength determined on the different porous samples. Initially, the introduction of 8 vol% of the porous agent during atomization leads to an increase of mechanical strength (≈580 ± 80 MPa if compared to around 290 ± 90 MPa for the denser sample). Subsequently, the strength decreases on further addition of porous agent, and reaches just less than its initial value at 27% of total porosity. Bending strength remains at a similar value of 85 ± 5 MPa on initial introduction of 8 vol% starch and then decreases to 42 ± 2 MPa as total porosity increases from 8% up to 27.5%. Variation of toughness as a function of porosity is presented in Fig. 12 which also shows a plot of calculated critical flaw size (after Griffith's equation) with porosity. The introduction of porous agent has a slight effect with a decrease in toughness from 1.12 ± 0.02 to ≈0.82 ± 0.05 MPa $\sqrt{m}$ at 14 vol% porosity. With 27.5 vol% porosity the overall toughness decreases from 1.12 ± 0.02 to 0.5 ± 0.04 MPa$\sqrt{m}$. A slight stabilization is observed just before the percolation threshold. The critical flaw size values do not vary significantly indicating that the porosity introduced by the starch is fully dispersed and still fine with no possibility of aggregation and remains constrained by only the size of the pore-forming agent (11 μm) which is well below the critical defect size in the matrix.

5. Discussion

In this work, with the chosen processing parameters, the clay–silica–feldspar starting material is not fully densified. Porosity is mainly closed. The observed mechanical properties have been explained in terms of catastrophic rupture initiated by larger pores. These specific pores result from the partial collapse of atomized spheres during shaping which are then not totally eliminated during sintering. Two routes of porous agent incorporation were investigated. For the One-step route, remarkably, compression strength is relatively stable when some porous agent is added. At the same time, a decrease is observed in flexural strength. Some explanation may be postulated that a lubricating effect occurs during pressing of the porous agent, which is viscoplastic, allowing a better collapse of granules. This seems consistent with SEM observations. A small amount of this porous agent decreases the initial critical flaw size and thus improves the mechanical properties of the more porous matrix. Nevertheless, this processing route does not lead to the formation of very fine and homogeneous microstructures. The percolation threshold appears at a low value (4%) of added porous agent ensuring a limited lightness (13% total porosity). For this value, mechanical properties are similar to the ceramic without pore forming agent but standard deviation is higher. For the Two-step route, involved an atomization step, the obtained microstructures are finer and more homogeneous. As a consequence, percolation threshold occurs at a significantly higher amount of porous agent (12%) and a slightly higher total porosity (16%) is obtained with a slight decrease of mechanical properties. In addition, the mechanical properties are maintained close to those of the matrix with mass reductions of 10%.

6. Conclusion

The mechanical properties of tableware ceramics are dependent on the size of the larger pores present in the part, which act as critical defects and initiate the catastrophic rupture of the material. Then it is possible to lighten these materials if the introduced porosity does not interact with the initial porosity and does not participate in the increase in the size of critical defects. A specific porous agent and a specific route of introduction have been specifically chosen to procure the generation of new porosity independent of the initial pores. For that, the clay–silica–feldspar raw powder and the porous agent are finely mixed and dispersed together in a slurry prior to atomization. The conditions of atomization are specifically adapted in order to ensure the integrity of the porous agent. By using this technique, it has been shown that it is possible to introduce new type of pores allowing up to 10% reduction in weight. As a consequence, mechanical properties are only slightly modified. As this work constitutes a first attempt, even lighter ceramics may be obtained by modifying the processing parameters and/or by changing the porous agent. In addition, some better characterization in terms of microstructure definition and mechanical properties and their mutual interaction will be useful to analyze more closely the mechanical behavior of these lighter materials. From an industrial viewpoint, the change would only focus on the powder synthesis step. Then it would be fully compatible with an industrial production process.

Acknowledgments

The authors gratefully acknowledge the support of the present research work by International Campus on Safety and Intermodality in Transportation, Nord-Pas-de-Calais Region France, European Community, Regional Delegation for Research and Technology, and the French Ministry of Higher Education and Research.

References

[1] D. Eliche-Quesada, C. Martínez-García, M. Martínez-Cartas, M. Cotes-Palomino, L. Pérez-Villarejo, N. Cruz-Pérez, F. Corpas-Iglesias, The use of different forms of waste in the manufacture of ceramic bricks, Applied Clay Science 52 (3) (2011) 270–276.

[2] S. Rhee, Porosity–thermal conductivity correlations for ceramic materials, Materials Science and Engineering 20 (1975) 89–93.

[3] B. Nait-Ali, K. Haberko, H. Vesteghem, J. Absi, D. Smith, Preparation and thermal conductivity characterisation of highly porous ceramics: comparison between experimental results, analytical calculations and numerical simulations, Journal of the European Ceramic Society 27 (2–3) (2007) 1345–1350.

[4] J.G. Ten, M. Orts, A. Saburit, G. Silva, Thermal conductivity of traditional ceramics. Part 1: influence of bulk density and firing temperature, Ceramics International 36 (6) (2010) 1951–1959.

[5] O. Lyckfeldt, J.M.F. Ferreira, Processing of porous ceramics by starch consolidation, Journal of the European Ceramic Society 18 (2) (1998) 131–140.

[6] Y. Sakka, F. Tang, H. Fudouzi, T. Uchikoshi, Fabrication of porous ceramics with controlled pore size by colloidal processing, Science and Technology of Advanced Materials 6 (8) (2005) 915–920.

[7] T. Moritz, H.-J. Richter, Ice-mould freeze casting of porous ceramic components, Journal of the European Ceramic Society 27 (16) (2007) 4595–4601.

[8] M. Descamps, T. Duhoo, F. Monchau, J. Lu, P. Hardouin, J. Hornez, A. Leriche, Manufacture of macroporous [beta]-tricalcium phosphate bioceramics, Journal of the European Ceramic Society 28 (1) (2008) 149–157.

[9] S.A. Barr, E. Luijten, Structural properties of materials created through freeze casting, Acta Materialia 58 (2) (2010) 709–715.

[10] F. Ye, J. Zhang, L. Liu, H. Zhan, Effect of solid content on pore structure and mechanical properties of porous silicon nitride ceramics produced by freeze casting, Materials Science and Engineering: A 528 (3) (2011) 1421–1424.

[11] Y. Kobayashi, E. Kato, Lightening of alumina-strengthened porcelain by controlling porosity, Journal of the Ceramic Society of Japan 106 (9) (1998) 938–941.

[12] A.K. Gain, H.-Y. Song, B.-T. Lee, Microstructure and mechanical properties of porous yttria stabilized zirconia ceramic using poly methyl methacrylate powder, Scripta Materialia 54 (12) (2006) 2081–2085.

[13] X. Mao, S. Wang, S. Shimai, Porous ceramics with tri-modal pores prepared by foaming and starch consolidation, Ceramics International 34 (1) (2008) 107–112.

[14] A. Diaz, S. Hampshire, Characterisation of porous silicon nitride materials produced with starch, Journal of the European Ceramic Society 24 (2) (2004) 413–419 (8th International Conference on Ceramic Processing).

[15] J. Martín-Márquez, J. Rincón, M. Romero, Effect of microstructure on mechanical properties of porcelain stoneware, Journal of the European Ceramic Society 30 (15) (2010) 3063–3069.

[16] Y. Zhang, L. Hu, J. Han, Z. Jiang, Freeze casting of aqueous alumina slurries with glycerol for porous ceramics, Ceramics International 36 (2) (2010) 617–621.
[17] D. Leguillon, R. Piat, Fracture of porous materials – influence of the pore size, Engineering Fracture Mechanics 75 (7) (2008) 1840–1853.
[18] T. Ohji, Microstructural design and mechanical properties of porous silicon nitride ceramics, Materials Science and Engineering: A 498 (1–2) (2008) 5–11.